Proc. Natl. Acad. Sci. USA
Vol. 76, No. 10, pp. 4842–4846, October 1979
Biochemistry

Origin of observed changes in ^{14}N hyperfine interaction accompanying R → T transition in nitrosylhemoglobin

(proximal imidazole/severe extension/cleavage)

S. K. MUN, JANE C. CHANG*, AND T. P. DAS

Department of Physics and Center for Biological Macromolecules, State University of New York at Albany, Albany, New York 12222

Communicated by George Feher, June 20, 1979

ABSTRACT **Theoretical investigations of electronic distributions in eight different structural forms of nitrosylhemoglobin were carried out to study the changes in ^{14}N hyperfine interaction observed with the transition from R to T structures under the influence of inositol hexaphosphate or changing pH. Four of the eight forms studied consisted of protonated and deprotonated N_{pros} in the proximal imidazole ligand with linear and bent Fe—N—O structures. Two other forms had a straight Fe—N—O structure and Fe—Im bond stretched by 0.5 and 1.0 Å. The other two systems we have studied are five-liganded NO-heme with bent and straight Fe—N—O structures. Our investigations show that arrangements of energy levels did not differ significantly among all the structures, the unpaired electron always occupying an antibonding orbital with d_z2 symmetry. The protonated and deprotonated systems with either linear or bent Fe—N—O structure showed substantial hyperfine interaction of the ^{14}N nuclei of the NO group and the N_ϵ atom of the proximal imidazole, indicating that a 9-line electron spin resonance hyperfine pattern (R structure) would be expected in all four cases. On the other hand, the extensions of the Fe—Im bond produce a sizeable decrease in the $^{14}N_\epsilon$ hyperfine interaction, indicating that an extension beyond 1.0 Å would provide a 3-line hyperfine pattern close to that found for the five-liganded NO-heme system. Our results thus provide quantitative support for the model of severe extension or cleavage of the Fe—N_ϵ bond proposed in the literature for explaining the R-to-T transition of the α-chain of nitrosylhemoglobin.**

The study of the properties of nitrosylhemoglobin (NO-Hb) has assumed major importance (1–4) in recent years for two main reasons. First, it is a six-liganded hemoglobin derivative that is paramagnetic with spin ½, which makes it amenable for electron paramagnetic resonance (EPR) studies (2–10). Such studies allow one to follow the changes in the electron distribution over the molecule associated with transitions between R and T states, considered to be of crucial importance in the explanation of cooperativity (11) in the oxygen-binding properties of hemoglobin. The second reason is that, in contrast to oxyhemoglobin and carbonmonoxyhemoglobin, NO-Hb shows a pronounced R-to-T transition (12, 13) in the presence of inositol hexaphosphate, this transition being also rather sensitive to changes (5, 9, 10) in pH of the surrounding environment. One of the properties of NO-Hb that is a sensitive indicator of changes of structure under the influence of inositol hexaphosphate or changes in pH is the splitting produced (3–10) in EPR spectra by ^{14}N hyperfine interactions. Thus, in NO-Hb A, in the presence of inositol hexaphosphate or at low pH one finds for the α chain a 3-line hyperfine pattern associated with the hyperfine interaction of the ^{14}N nucleus of NO. On increasing the pH beyond 8.0, even in the presence of inositol hexaphosphate one sees a change (5) from the 3-line to a 9-line pattern, indicating that there is now a sizeable hyperfine interaction also with the $^{14}N_\epsilon$ of the imidazole (Im) of the sixth ligand of iron, the proximal histidine. The β chain, on the other hand (6–9), always appears to remain in the high-affinity form with the unpaired electron interacting with the ^{14}N nuclei of both the NO and Im ligands. Other types of experimental data, such as the infrared frequencies (14) associated with NO group and the Soret, UV, and visible band frequencies and intensities, sulfhydryl reactivities, and (1, 15) exchangeable proton magnetic resonances are also found to undergo marked changes in the presence of inositol hexaphosphate. The nitrosyl derivative of hemoglobin Kansas (NO-Hb Kansas) seems to demonstrate (3, 5) the changes for the α-chain even more markedly than does NO-Hb A, the 3-line hyperfine pattern in EPR signals being retained in the presence of inositol hexaphosphate up to pH 8.5, beyond which one gets a 9-line pattern.

One of the models proposed (1) to explain the R-to-T transition and the corresponding changes in the EPR signals from 9-line to 3-line hyperfine patterns for the α-chain is that there is a severe weakening of the Fe—N_ϵ bond associated with the proximal Im, corresponding to a drastic extension of the bond or even a cleavage of the Im ligand. Support for this transition to an essentially five-liganded structure in the T state has been cited (2) from the comparison of the similarity (6–10) of the hyperfine patterns in the T state and in the five-liganded NO-heme system (16) and from the similarity (13) of the infrared frequencies for NO-heme and six-liganded NO-Hb in the T state under the influence of inositol hexophosphate. An alternative model that has been proposed (17) in the literature is that the change from the 9-line to the 3-line EPR signal may be associated with changes in the nature of the unpaired spin orbital due to differences in the arrangement of electronic levels for NO-Hb molecules when the N_{pros} of the proximal histidine ligand is in a protonated or deprotonated state. Additionally, it has also been proposed (3), from phenomenological analysis of the g-shift and the hyperfine interaction tensors, that the high-affinity R form corresponding to the 9-line EPR pattern is associated with the bent Fe—N—O structure with a bond angle of 105°, the 3-line pattern is associated with a linear Fe—N—O structure, the linearity of the Fe—N—O bond system leading to a marked weakening of the Fe-Im interaction.

We thought that at this stage, with substantial experimental data available, it would be helpful to test these models from an *ab initio* quantum mechanics point of view (17, 18). For this purpose, we have investigated the energy levels and electronic wave functions and associated hyperfine interaction energies

The publication costs of this article were defrayed in part by page charge payment. This article must therefore be hereby marked "*advertisement*" in accordance with 18 U. S. C. §1734 solely to indicate this fact.

Abbreviations: NO-Hb, nitrosylhemoglobin; EPR, electron paramagnetic resonance; SCCEH, self-consistent-charge extended Hückel; Im, imidazole.

* Present address: Singer Kearfott, 150 Totowa Road, Wayne, NJ 07470.

of the ^{14}N nuclei of NO and proximal histidine ligands in the different structures associated with the various models (1, 16) proposed for the NO-Hb molecules to explain the 9- and 3-line hyperfine patterns. Our results will be seen to lend quantitative support to the model of Fe—Im bond weakening or cleavage as the cause of the transition from the 9-line to the 3-line EPR hyperfine pattern in going from the R to the T state of NO-Hb.

PROCEDURE

For the study of the hyperfine interaction in the NO-Hb system in various atomic configurations, we need to obtain the corresponding electronic wave functions and use them to evaluate the perturbation energy, linear in the nuclear moment, arising out of the electron–nuclear hyperfine interaction Hamiltonian. The rigorous solution to the molecular Schrödinger equation is difficult to obtain even for the smallest molecular systems such as diatomic molecules because the wave function would have to include many-body effects explicitly. The next best procedure would be to use the one-electron approximation, including self-consistency, through a first-principle Hartree–Fock approach. This has been done in the literature for a number of diatomic molecules but would require a prohibitively large amount of effort for the large molecules of biological interest, such as the present one, NO-Hb. One therefore has to resort to approximate procedures which are simple enough to be practical for the present system but also have the basic physical features of the complicated self-consistent Hartree–Fock approach. A number of such approximation procedures are available in the literature, of which we have chosen the self-consistent-charge extended Hückel (SCCEH) approach (18–20). In this procedure, the molecular orbital wave-functions are expressed in the form:

$$\phi_\mu = \sum_i C_{\mu i} \chi_i \qquad [1]$$

in which the χ_i are atomic orbitals of the atoms in the system encompassing in our case the $3d$, $4s$, and $4p$ orbitals of the iron atoms, the $2s$ and $2p$ orbitals of carbon and nitrogen, and the $1s$ orbitals of hydrogen atoms. The variational parameters $C_{\mu i}$ and E_μ are obtained by solving the linear equations

$$\sum_j C_{\mu i}(H_{ij} - S_{ij}E_\mu) = 0 \qquad [2]$$

In contrast to the Hartree–Fock procedure, in which the matrix elements H_{ij} are obtained from first principles, in the SCCEH procedure they are related to the ionization energies $E_i{}^0$ and $E_i{}^\pm$ of the neutral atoms and ions by

$$H_{ii} = E_i{}^0 \pm |q_l|(E_i{}^\pm - E_i{}^0) \qquad [3]$$

$$H_{ij} = \frac{K}{2} S_{ij}(H_{ii} + H_{jj}) \qquad [4]$$

in which S_{ij} is the overlap integral involving the atomic orbitals χ_i and χ_j and K is a semi-empirical parameter obtained by fitting the separation between molecular energy levels and observed spectra in a number of porphyrin and metal–porphyrin systems and found to lie in the range 1.75–2.00 with 1.89 (18) appearing to be the most satisfactory choice. Although this method is not completely self-consistent as in the Hartree–Fock procedure, partial self-consistency is introduced through the dependence of H_{ii} (and therefore H_{ij}) in Eq. 3 through the atomic charges q_l related to the coefficients $C_{\mu i}$ in Eq. 1 through the Mulliken approximation (21). Although this method is semi-empirical because of the assumptions made in the equations for the Hamiltonian matrix elements, it is thought that it has the potential of providing energy levels and electron distributions with physical features corresponding to those obtainable from more rigorous Hartree–Fock calculations because of the incorporation of partial self-consistency through the charges q_l, the use of experimental atomic ionization energies, and the explicit incorporation of overlap effects between the penetrating tails of the atomic wave functions on neighboring centers through S_{ij} in Eq. 4. This expectation has been found to be borne out through overall satisfactory agreement (22, 23) between theory and experiment for spectroscopic data in a number of metal–porphyrins and a number of properties related explicitly to the electronic wave functions such as hyperfine constants of iron (22) and other nuclei such as ^{14}N (22) and halogen (24) nuclei, electron spectroscopy for chemical analysis (ESCA) (25), and isomer shift (26) data in a number of high-spin five-liganded and six-liganded heme systems.

We have carried out calculations for both the five-liganded system with NO as the fifth ligand and the six-liganded systems with the Im of the proximal histidine as the sixth ligand. We have used available x-ray structural data on the five-liganded (27) and six-liganded (28) compounds NO-Fe-TPP and NO-Fe-TPP-MeIm (TTP, tetraphenylporphyrin), with bent Fe—N—O configuration, for choosing the positions of iron and the orientations of the NO and Im groups. Thus, the Fe atom was chosen to lie 0.211 and 0.07 Å above the porphyrin plane, toward the NO group, in the five- and six-liganded systems, respectively. The bond angles in the bent Fe—N—O configuration in the five- and six-liganded cases were 149.2° and 142.1°, respectively, and the planes of the Fe—N—O bond and Im were chosen to be coplanar (Fig. 1). For the straight Fe—N—O configurations that we have studied, the other parameters were kept the same as in the bent configurations with only the NO bond made collinear with the Z axis, the direction perpendicular to the porphyrin plane. For the extended Fe—Im bond situations, the Fe—N distances in Fig. 1 were extended beyond the values in the model compounds (27, 28) for which x-ray data are available, by 0.5 and 1.0 Å, respectively. The calculations were carried out with both protonated and deprotonated Im ligand, corresponding to the exchangeable proton attached to N_{pros} (where a CH_3 group is attached in the model compounds), either present or removed. As in earlier work (19, 24) with other heme systems, all the side chains of the

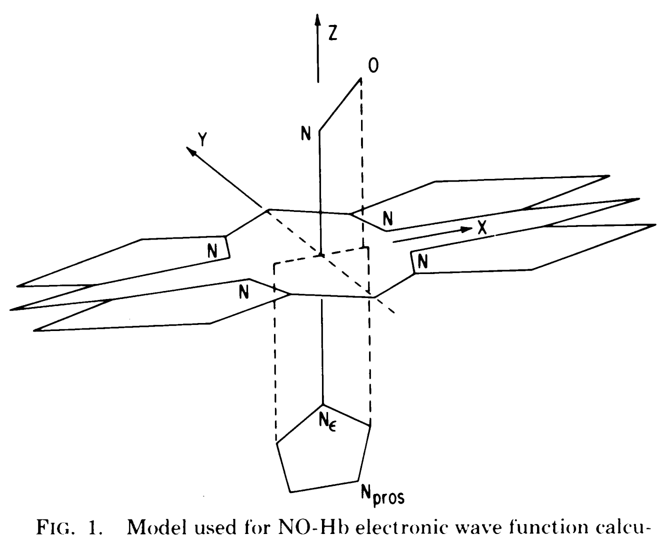

FIG. 1. Model used for NO-Hb electronic wave function calculation. The positions of the atoms are based on those for NO—Fe—TPP—MeIm (TTP = tetraphenylporphyrin), as explained in the text. The angle of N—O with the perpendicular to the heme plane and the Fe—N_ϵ distances are varied for the different structures studied.

pyrroles of the porphyrin ring were replaced by hydrogen to avoid excessive computational effort. This replacement is not expected to have any significant effect on the electron distributions of the N atom ligands of Fe in which we are primarily interested.

For studying nuclear hyperfine interactions with the calculated wave functions, we need to obtain the expectation values of the electron–nuclear hyperfine interaction Hamiltonian in Eq. **5** involving the contact and dipolar terms, respectively (29).

$$\mathcal{H}_{eN} = \frac{8\pi}{3}\gamma_e\gamma_N\hbar^2\sum_i \vec{I}_N\vec{s}_i\delta(\vec{r}_i) + \gamma_N\gamma_e\hbar^2[3(\vec{s}_i\cdot\vec{r}_i)(\vec{I}_N\cdot\vec{r}_i) - r_i^2(\vec{I}_N\cdot\vec{s}_i)]/r_i^5].$$

With the molecular orbital wave functions in Eq. **1**, the isotropic and anisotropic hyperfine components A and $\vec{B}$ of the spin-Hamiltonian

$$\mathcal{H}_{spin} = A\vec{I}\cdot\vec{S} + \vec{I}\cdot\vec{B}\cdot\vec{S} \qquad [6]$$

for any particular ^{14}N nucleus are given by (13)

$$A = \frac{8\pi\gamma_e\gamma_N\hbar^2}{6S}|\phi_\mu(N)|^2 \qquad [7]$$

and

$$B_{ij} = \frac{\gamma_e\gamma_N\hbar^2}{2S}\left\langle\frac{1}{r^3}\right\rangle_{2p}\sum_{ij}\left(\frac{2}{5}\right)(3C_{\mu i}C_{\mu j} - \sum_k C_{\mu k}^2\delta_{ij}) \qquad [8]$$

in which μ refers to the unpaired spin orbital $S = \frac{1}{2}$ and i, j, and $k = 1, 2, 3$ refer to the $2p_x$, $2p_y$, and $2p_z$ N orbital components of the unpaired spin orbital. The contribution to A from $|\phi_\mu(N)|^2$ arises mainly from the N atom component in the unpaired spin orbital although there can be some contributions from the tails of orbitals on neighboring atoms (19, 24). In addition to the direct contributions to A and $\vec{B}$ given by Eqs. **7** and **8**, there can be some contributions from the exchange polarization effect (19, 24) on the paired-spin orbitals including the core-orbitals by the unpaired spin orbital. The possible importance of the exchange polarization effect for NO-Hb systems will be remarked on in the next section where our results for the hyperfine interaction are discussed and compared with experimental data. The calculated dipolar hyperfine tensor has been diagonalized to obtain the principal axis component, $B_{z'z'}$, referring to the maximal component in the principle axis system.

RESULTS AND DISCUSSIONS

In Table 1, the values of the contact contribution A to the hyperfine constant of ^{14}N, the maximal component $B_{z'z'}$ of the dipolar hyperfine tensor in the principle axis system, and the sum of the two are listed for the different configurations of the heme and its NO and Im ligands in NO-Hb that we have studied. The sums $A + B_{z'z'}$ are expected to be representative of the extents of hyperfine splitting of the electron spin resonance signal produced by the various ^{14}N nuclei.

The first significant feature in our results is that the hyperfine fields are substantially smaller at the ^{14}N nuclei for the porphyrin nitrogens than for N_{NO} and N_ϵ from the fifth and sixth ligands of Fe, being <3 gauss for all the cases considered. The corresponding hyperfine field for the N_{pros} of the Im ligand is even smaller, <1 gauss. This feature of our results explains the fact that the number of hyperfine lines observed is never more than nine, associated with the relatively strong hyperfine interactions arising from $^{14}N_{NO}$ and $^{14}N_\epsilon$. It would be interesting to have experimental results for these weak hyperfine interactions for the porphyrin nitrogens and N_{pros} in the future, perhaps by ENDOR measurements, to compare with predictions of theory.

The next important feature of our results is that protonation and deprotonation of N_{pros} alone with either bent or linear Fe—N—O structure cannot explain the transition in the hyperfine structure of the EPR signal from a 9- to a 3-line pattern, because the ratios of the ^{14}N hyperfine fields at N_{NO} and N_ϵ sites are comparable for the systems with protonated and deprotonated N_{pros}. The third feature of our results is that a change in Fe—N—O bond angle, such as between the straight and bent bonds in our work, without any additional changes in the molecule cannot explain the transition in the hyperfine splitting from the 9- to the 3-line pattern. The latter feature and the preceding one was expected from our result for the arrangements of energy levels in the four cases of bent and linear Fe—N—O bonds combined with protonated and deprotonated N_{pros}. The arrangements for all four cases did not show any significant variations, with the unpaired electron always occupying the d_z2 orbital.

In view of these results indicating the inability of the previous four cases to provide any significant trends toward the change to the 3-line pattern from the 9-line pattern, we studied the influence of Fe—N_ϵ bond extension on the electronic structure and spin-distributions over the molecule. The hyperfine parameters obtained for the structure involving Fe—N_ϵ extensions of 0.5 and 1.0 Å listed in Table 1 bring us to the next and perhaps the most important feature of our results. With the extension of the Fe—N_ϵ ligand by 0.5 Å, there is a substantial decrease in $A + B_{z'z'}$ for $^{14}N_{NO}$, the decrease being further

Table 1. Calculated ^{14}N hyperfine coupling constants (gauss)

NO-Hb*	$^{14}N_{NO}$ A	$^{14}N_{NO}$ $B_{z'z'}$	$^{14}N_{NO}$ $A + B_{z'z'}$	$^{14}N_\epsilon$ A	$^{14}N_\epsilon$ $B_{z'z'}$	$^{14}N_\epsilon$ $A + B_{z'z'}$
Bent Fe—N—O						
NO-Hb (p)	12.51	6.92	19.43	10.16	5.03	15.19
NO-Hb (d)	12.32	6.72	19.04	10.76	5.62	16.38
NO-heme	8.79	7.04	15.83	—	—	—
Linear Fe—N—O						
NO-Hb (p)	20.42	1.67	22.09	12.74	6.63	19.37
NO-Hb (d)	19.74	1.60	21.34	13.94	8.00	21.94
NO-heme	12.66	1.30	13.96	—	—	—
Fe—N_ϵ (0.5 Å)†	17.02	1.54	18.56	7.68	4.34	12.02
Fe—N_ϵ (1.0 Å)†	12.83	1.17	14.00	3.48	1.23	4.71

* p and d refer to protonated and deprotonated N_{pros} in proximal Im.
† Fe—N_ϵ bond length extended by 0.5 and 1.0 Å.

accentuated for the extension by 1.0 A. From the decrease in $A + B_{z'z'}$, it appears that a weakening of the Fe—N_ϵ bond described by a small additional extension beyond 1.0 Å should produce a virtually negligible hyperfine interaction for $^{14}N_\epsilon$, analogous to the completely severed Fe—N_ϵ bond situation represented by the five-liganded NO-heme system with linear Fe—N—O structure.† For the NO-Hb structures considered, the energy level arrangements show consistently that the unpaired electron occupies the antibonding d_z2 type molecular orbital (1), the decrease in the $^{14}N_\epsilon$ hyperfine interaction being primarily a result of the weakening of the Fe—N_ϵ bonding, involving a decreased amount of N_ϵ orbital admixtures in the d_z2-type molecular orbital.

Another notable feature of our results is that the $^{14}N_{NO}$ hyperfine interaction constant is smaller in the completely severed five-liganded NO-heme system than in the six-liganded case, in keeping with experimental observation (2, 9) in this respect. Furthermore, the $^{14}N_{NO}$ hyperfine interaction decreases continuously as the Fe—N_ϵ bond is weakened progressively by extension. It is difficult to pinpoint an exact physical explanation of this trend in view of the complexity of the present system. However, our molecular orbital calculation does show that the unpaired spin d_z2-like orbital gets more localized on the Fe atom when the Fe—N_ϵ bond is extended. It appears then that, instead of competing with each other, the two Fe—N bonds involving the bonding of Fe to the NO and Im ligands actually act in unison in causing delocalization of the Fe d_z2 orbital, which can be interpreted as a *trans* effect of one ligand on the other.

The results in Table 1 show another interesting feature. Thus, in the cases in which we have carried out calculations for both linear and bend Fe—N—O structures, although the net hyperfine constants $A + B_{z'z'}$ are close to each other, they are composed of differing proportions of A and $B_{z'z'}$. In particular, the isotropic term A appears to be larger for the linear case and $B_{z'z'}$ is smaller in this case. Both these trends perhaps can be understood from a consideration of the nature of the bonding between the d_z2 orbital of Fe and the orbitals of the NO ligand. Thus, in the linear Fe—N—O structure, the d_z2 orbital is collinear with an orbital of NO involving a hybrid of s and p orbitals on N. Consequently, there is significant N atom s character admixed in the unpaired molecular orbital. For the bent case, however, there can be a bonding of the Fe d_z2 orbital with both the σ and π orbitals of NO. Because the latter does not involve s character on the N atom, it is understandable that the net amount of s character in the unpaired molecular orbital is decreased in the bent Fe—N—O case. The consequent increase in the amount of N p character in the unpaired molecular orbital could also explain the larger dipolar interaction in the bent Fe—N—O cases.

† The sizeable extension required for decreasing the ^{14}N hyperfine interaction substantially enough to obtain a 3-line hyperfine pattern is a consequence of the diffuseness of the Fe $3d_z2$ orbital. This makes the overlap between the latter orbital and the nitrogen $2s$ and $2p_z$ orbitals, and consequently the corresponding off-diagonal matrix elements given by Eq. 4, rather slowly varying, requiring a significant extension before the bonding between the Fe $3d_z2$ and N orbitals can become vanishingly small. It is interesting that Scheidt *et al.* (30) have found that an extension of only 0.45 Å in the Fe—N_ϵ bond appears to change the NO stretching frequency from that characteristic of the six-liganded system to that of the five-liganded system, an extension of less than half of what is found to be needed from the present work to make the $^{14}N_\epsilon$ hyperfine interaction unobserverably small. These relative rates of variation of the NO stretching frequency and $^{14}N_\epsilon$ hyperfine interaction support the conclusion reached recently by Hoffman and coworkers (31) that the NO stretching frequency is a better operational indicator of R-to-T transition in NO-Hb than is the splitting of the EPR spectra.

It should be noted that although there seems to be satisfactory agreement between theory and experiment for the hyperfine splitting associated with $^{14}N_{NO}$ there are some differences in the magnitudes of the $^{14}N_\epsilon$ hyperfine constants in the 9-line case between the calculated results in Table 1 and experimental results (2–10). The experimental splittings suggest a hyperfine interaction constant between 6 and 8 gauss whereas our results for A are between 10 and 13 gauss and for $A + B_{z'z'}$ they are between 15 and 22 gauss. One possible source for this difference could be a deviation in the atomic arrangement from the ideal symmetric arrangement shown in Fig. 1. In fact, x-ray data (30) on model systems involving the MeIm ligand show small deviations of the linearity of Fe—N_ϵ bond with respect to the Fe—N_{NO} bond. Similar deviation in the Fe—N_ϵ bond orientation as well as tilting of the Im plane have been seen for these model systems as well as in met-myoglobin (32). Additionally, there is a deviation in the azimuthal angle of the Im plane by about 3.9° in the model MeIm compound from that shown in Fig. 1. We have tested the influence of the first two departures from the idealized structure in Fig. 1 by bending the Fe—N_ϵ bond and tilting the Im plane and find that bending and tilting angles of about 10° can produce decreases in the $^{14}N_\epsilon$ hyperfine interaction in the right direction for comparison with experiment but not enough to make the value as small as the 6–8 gauss observed experimentally. A second possible source for this difference is the exchange polarization effect that has been found (24) to have significant influence on the magnitudes of the porphyrin and Im ^{14}N hyperfine constants in high-spin heme compounds and methemoglobin systems. It will be helpful in the future to study these effects in NO-Hb quantitatively (33) to see how they influence both the $^{14}N_{NO}$ and $^{14}N_\epsilon$ results. It would also be helpful to study the ^{14}N hyperfine interactions by other procedures for obtaining the electronic wave functions.

Our investigation of the energy levels, wave functions, and ^{14}N hyperfine interactions for different configurations of the α-chain of NO-Mb including protonated and deprotonated Im in the proximal histidine, bent and straight Fe—N—O orientations, and sizeable extensions (0.5–1.0 Å) of the Fe—N_ϵ bond to the proximal Im lead to the following conclusions.

(*i*) The protonation and deprotonation of N_{pros} in the Im of the proximal histidine ligand does not influence the $^{14}N_{NO}$ and $^{14}N_\epsilon$ hyperfine constant significantly‡ and cannot explain the observed change from a 9- to a 3-line hyperfine pattern in the EPR spectrum accompanying the R-to-T transition.

(*ii*) The change in Fe—N—O bond angle associated with bent and straight orientations of NO produces small changes in the net $^{14}N_{NO}$ and $^{14}N_\epsilon$ hyperfine constants which are not substantial enough to explain the observed changes from a 9- to a 3-line hyperfine pattern in the EPR spectrum.

(*iii*) The extensions of the Fe—N_ϵ bond, however, do produce a significant decrease of the ^{14}N hyperfine constant and indicate that beyond 1.0-Å extension, one can explain the observed 3-line pattern for the T system which is associated with only the $^{14}N_{NO}$ hyperfine interaction.

‡ The N_{pros} hyperfine interaction constant does show a somewhat more significant change from ≈0.65 to 0.99 gauss in going from the protonated to the deprotonated case in the linear Fe—N—O bond situation, the change being less marked for the bent Fe—N—O bond situation. However, these differences are difficult to observe in view of the small sizes of these hyperfine constants. There is a substantially more important change in the charge on the N_{pros}, from about −0.06 in the protonated system to close to −0.34 in the deprotonated system. This negative charge, however, arises mainly from changes in the N_{pros} atomic orbital population associated with paired molecular orbitals characteristic of Im.

Thus, our results provide theoretical support for the model of dramatic bond weakening produced by severe extensions and even cleavage of the Fe-Im bond proposed (1) to explain the R-to-T transition (12, 13) in NO-Hb manifested through several observed properties under the influence of IHP.

This work was supported by grants from the National Heart and Lung Institute and the General Medicine Division of the National Institutes of Health.

1. Perutz, M. F., Kilmartin, J. V., Nagai, K., Szabo, A. & Simon, S. R. (1976) *Biochemistry* **15,** 378–387.
2. Szabo, A. & Perutz, M. F. (1976) *Biochemistry* **15,** 4427–4428.
3. Dickinson, L. C. & Chien, J. C. W. (1971) *J. Am. Chem. Soc.* **93,** 5036–5040.
4. Chien, J. C. W. & Dickinson, L. C. (1977) *J. Biol. Chem.* **252,** 1331–1335.
5. Chevion, M., Stern, A., Peisach, J., Blumberg, W. E. & Simon, S. (1978) *Biochemistry* **17,** 1745–1750.
6. Rein, H., Ristau, O. & Scheler, W. (1972) *FEBS Lett.* **24,** 24–26.
7. Kon, H. (1968) *J. Biol. Chem.* **243,** 4350–4357.
8. Kon, H. & Kataoka, N. (1969) *Biochemistry* **8,** 4757–4762.
9. Henry, Y. & Banerjee, R. (1973) *J. Mol. Biol.* **73,** 469–482.
10. Nagai, K., Hori, H., Yoshida, S., Sakamoto, H. & Morimoto, H. (1978) *Biochim. Biophys. Acta* **532,** 17–28.
11. Perutz, M. F. (1978) *Sci. Am.* **239,** 68–86.
12. Salhany, J. M., Ogawa, S. & Shulman, R. G. (1975) *Biochemistry* **14,** 2180–2190.
13. Maxwell, J. C. & Caughey, W. S. (1976) *Biochemistry* **15,** 388–396.
14. Sharma, V. S. & Ranney, H. M. (1978) *J. Biol. Chem.* **253,** 6467–6472.
15. Salhany, J. M., Ogawa, S. & Shulman, R. G. (1974) *Proc. Natl. Acad. Sci. USA* **71,** 3359–3362.
16. Wayland, B. B. & Olson, L. W. (1974) *J. Am. Chem. Soc.* **96,** 6037–6041.
17. Peisach, J. (1975) *Ann. N.Y. Acad. Sci.* **244,** 187–203.
18. Zerner, M., Gouterman, M. & Kobayashi, H. (1966) *Theor. Chim. Acta* **6,** 363–400.
19. Han, P. S., Rettig, M. F. & Das, T. P. (1970) *Theor. Chim. Acta* **16,** 1–21.
20. Hoffman, R. (1963) *J. Chem. Phys.* **39,** 1397–1412.
21. Mulliken, R. S. (1955) *J. Chem. Phys.* **23,** 1833–1841.
22. Mun, S. K., Chang, J. C. & Das, T. P. (1977) *Biochim. Biophys. Acta* **490,** 249–253.
23. Mallick, M. K., Mun, S. K., Mishra, S., Chang, J. C. & Das, T. P. (1978) *Hyperfine Interact.* **4,** 914–920.
24. Mallick, M. K., Chang, J. C. & Das, T. P. (1978) *J. Chem. Phys.* **68,** 1462–1473.
25. Mun, S. K., Chang, J. C. & Das, T. P. (1979) *J. Am. Chem. Soc.*, in press.
26. Chang, J. C., Kim, Y. M., Das, T. P. & Duff, K. J. (1976) *Theor. Chim. Acta* **41,** 37–49.
27. Piciulo, P. L., Rupprecht, G. & Scheidt, W. R. (1974) *J. Am. Chem. Soc.* **96,** 5293–5295.
28. Scheidt, W. R. & Frisse, M. E. (1975) *J. Am. Chem. Soc.* **97,** 17–21.
29. Das, T. P. (1973) *Relativistic Quantum Mechanics of Electrons* (Harper and Row, New York), p. 184.
30. Scheidt, W. R., Brinegar, A. C., Ferro, E. B. & Kirner, J. F. (1977) *J. Am. Chem. Soc.* **99,** 7315–7322.
31. Scholler, M. Y., Wang, R. & Hoffman, B. M. (1979) *J. Biol. Chem.* **254,** 4072–4078.
32. Takano, T. (1977) *J. Mol. Biol.* **110,** 537–568.
33. Ikenberry, D., Rao, B. K., Mahanti, S. D. & Das, T. P. (1969) *J. Magn. Reson.* **1,** 221.